CrystEngComm

PAPER

View Article Online
View Journal | View Issue

Check for updates

Cite this: *CrystEngComm*, 2022, **24**, 7632

Design of coordination polymers based on combinations of 1,2-diphenylethane-1,2-diyl diisonicotinate with Cu(II), Zn(II), Cd(II) and Co(II)†

Sofia Zazouli,[a] Nathalie Gruber, [b] Véronique Bulach, *[b] Sylvie Ferlay *[b] and Abdelaziz Jouaiti *[b]

Received 22nd July 2022,
Accepted 7th October 2022

DOI: 10.1039/d2ce01001a

rsc.li/crystengcomm

Five new supramolecular coordination polymers (**L**-Cu(acac)$_2$, **L**-Cu(hfac)$_2$, **L**-ZnCl$_2$, **L**-CdI$_2$ and **L**-CoCl$_2$) based on the use of the flexible organic ligand **L** (1,2-diphenylethane-1,2-diyl diisonicotinate) combined with Cu(acac)$_2$, Cu(hfac)$_2$, ZnCl$_2$, CdI$_2$ or CoCl$_2$ metallaligands, were synthesized and structurally characterized by single-crystal X-ray diffraction. They represent the first reported coordination polymers based on this ligand presenting ester junctions. X-ray diffraction analysis revealed the structure and the dimensionality of these coordination polymers as well as their packing in the crystal that depends on the conformation adopted by the ligand **L** and the nature of the used metallic salts.

Introduction

During the past two decades, there has been a huge number of reports in the field of Coordination Polymers (CPs).[1–5] The building of CPs involves supramolecular architectures based on the self-assembly of organic ligands and metal ions linked by coordination bonds, with specific directionality. Different dimensionalities have been described for these molecular networks, from one-dimensional simple chains, to more sophisticated architectures, and up to three-dimensional networks, showing a strong dependency on the choice of the metal ions, ligand, anions, and solvents used for the formation of CPs in the solid state.[6–10] The incorporation of functional properties at the level of the metal centers or in the backbone of the organic linkers has allowed the development of different applications in the field of catalysis, gas storage, luminescence, and sensing, among others.[11–17]

The development of the crystal engineering strategy in this field has enabled the possibility to obtain and elucidate a multitude of crystalline structures presenting different topologies.[18–21] To achieve some predictability of the molecular structures, a certain degree of structural rigidity for the used molecular building blocks is required. Unlike rigid organic ligands, which display no free rotation around the chemical bonds that could orient the coordinating groups,[22–24] flexible ligands behave as multi directional, which allows them to propose different conformations leading to different coordination orientations, when combined with a metal cation. This type of ligands may produce a large variety of structures in the solid state, because of their ability to bend or turn around bonds and orient themselves differently towards metals during the crystallization process in solution.[25–27]

A large variety of flexible ligands are available, and, for example, the neutral ligand ethanediyl bis(isonicotinate), has been used for the formation of coordination polymers of various dimentionalities.[28–33] Due to its flexible nature, this ligand displays several coordination possibilities by forming thus metallamacrocycles[28–31] and CPs,[32,33] when combined with a metallic salt. Depending on the experimental conditions, this flexible ligand adopts an *anti* or *syn* conformation in the crystalline state. Another example of ligand belonging to this family is 1,2-diphenylethane-1,2-diyl diisonicotinate, with ester junctions, (**L**, Scheme 1), for which only its crystalline structure in the solid state has been

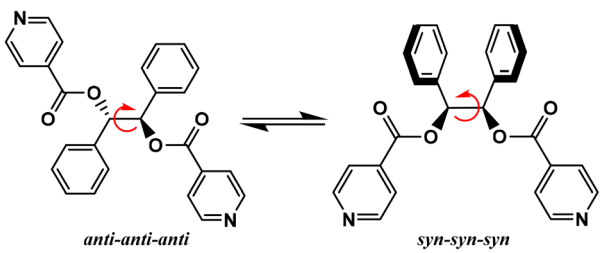

Scheme 1 Two possible conformations for 1,2-diphenylethane-1,2-diyl diisonicotinate (**L**).

[a] *Laboratoire de Développement Durable, Faculté des Sciences et Techniques, Université Sultan Moulay Slimane, B.P. 523, 23000 Beni Mellal, Morocco*
[b] *CNRS, CMC UMR 7140, Université de Strasbourg, F-67000 Strasbourg, France. E-mail: ferlay@unistra.fr, jouaiti@unistra.fr*

† CCDC 2189978–2189982. For crystallographic data in CIF or other electronic format see DOI: https://doi.org/10.1039/d2ce01001a

Open Access Article. Published on 07 oktober 2022. Downloaded on 26.04.2026 03.20.59.
This article is licensed under a Creative Commons Attribution-NonCommercial 3.0 Unported Licence.

This journal is © The Royal Society of Chemistry 2022

Open Access Article. Published on 07 oktober 2022. Downloaded on 26.04.2026 03.20.59.
This article is licensed under a Creative Commons Attribution-NonCommercial 3.0 Unported Licence.

reported.[34] **L** is a synthetic ditopic ligand composed of two phenyl and two pyridine moieties, that, to the best of our knowledge, has never been described in a coordination polymer. This ditopic ligand possesses a free rotation around the ethylene bond, which could enable different orientations of the pyridine coordinating entities. This allows to generate a large variety of polymeric structures with different dimensionalities by combining **L** with metal cations. For this ligand, two limit conformations could be observed in solution: the *anti-anti-anti* and *syn-syn-syn* (Scheme 1).

The analog of **L**, *N*,*N*′-(1,2-diphenylethane-1,2-diyl)-diisonicotinamide, a ligand involving amide junctions (instead of esters for **L**) has been investigated by Sadegh *et al.* a decade ago,[35] and two molecular isostructural coordination polymers based on Hg(II) were reported. In these polymeric compounds, the ligand adopts an *anti-anti-anti* conformation, with the participation of the pyridine as well as the carbonyl groups in the coordination with the Hg(II) cations.

Herein, we report the preparation procedure and characterization of **L** and the structures of the obtained coordination polymers when **L** is combined with $Cu(acac)_2$, $Cu(hfac)_2$, $ZnCl_2$, CdI_2 or $CoCl_2$ salts. We focused on the use of divalent metal ions presenting different coordination geometries (mainly octahedral and tetrahedral), that could also be influenced by the nature of the counter anion. Thus, the metal complexes $Cu(acac)_2$ and $Cu(hfac)_2$ act as a linear connectors, while $ZnCl_2$ and CdI_2 adopt a V-shape and $CoCl_2$ behaves as a square shaped assembling node. Five new supramolecular coordination polymers based on the combination of **L** with $Cu(acac)_2$, $Cu(hfac)_2$, $ZnCl_2$, CdI_2 or $CoCl_2$ salts are here reported and their structures have been discussed.

Results and discussion

Synthesis of L

The synthesis of **L** was achieved at room temperature upon treatment of *meso*-1,2-diphenyl-1,2-ethanediol with commercially available isonicotinoyl chloride, as its hydrochloride salt in dry THF, and in the presence of Et_3N. **L** is obtained in 77% yield and has been characterized by ^1H and ^{13}C NMR in solution together with elemental analysis (see Experimental part).

Formation of CPs

The corresponding CPs were synthesized under mild reaction conditions. A solution of $Cu(acac)_2$, $Cu(hfac)_2$, $ZnCl_2$, CdI_2 or $CoCl_2$ in EtOH was carefully layered on a solution of **L** in $CHCl_3$. After three days, crystals of **L-Cu(acac)$_2$**, **L-Cu(hfac)$_2$**, **L-ZnCl$_2$**, **L-CdI$_2$** and **L-CoCl$_2$**, single-crystal suitable for X-ray diffraction analysis were collected (see Experimental part). For all the described compounds, the bond lengths values found in **L** are in accordance with those previously reported[34] and are not discussed here below.

Structural description for 1D CPs L-Cu(acac)$_2$ and L-Cu(hfac)$_2$

Combination of $Cu(acac)_2$ or $Cu(hfac)_2$ with **L** leads in both cases, to bluish-green crystalline materials after a few days. As expected, combinations of **L** with two different Cu(II) metallaligand, $Cu(acac)_2$ (or $Cu(hfac)_2$), behaving both as two-connected linear connector, leads to similar neutral 1D coordination polymers (**L-Cu(acac)$_2$** and **L-Cu(hfac)$_2$**), as revealed by the X-ray diffraction study on single crystals. **L-Cu(acac)$_2$** and **L-Cu(hfac)$_2$** result from the bridging of consecutive ligands **L** by $Cu(acac)_2$ (or $Cu(hfac)_2$) complexes, respectively. Both isomorphous coordination polymers crystallize in the monoclinic $P2_1/n$ space group (see the crystallographic data in Table 1) and their asymmetric unit is composed of one ligand **L**, one Cu^{2+} cations and two $acac^-$ (or $hfac^-$) anions. For **L-Cu(hfac)$_2$**, disorder has been found for the F atoms present in $hfac^-$ anion. It should be noted, that in both coordination polymers, there are no solvent molecules in the lattice.

The copper(II) metal center displays distorted octahedral coordination geometry. The four equatorial positions are occupied by four oxygen atoms (from the two $acac^-$ or $hfac^-$ anions) and two nitrogen atoms from pyridine moieties, occupied the two axial positions, as shown in Fig. 1. As shown in Table 2, the Cu–O or Cu–N bond lengths values are usual for Cu(II) cations ranging from 1.93 to 2.48 Å in **L-Cu(acac)$_2$** and from 1.99 to 2.26 Å in **L-Cu(hfac)$_2$** (Table 2).

The pyridine and the phenyl units of the ligand in both CPs adopt an *anti* orientation, as already observed for the ligand alone in the solid state,[34] and are roughly perpendicular to each other.

In the crystal, the chains are running along the *a* axis for **L-Cu(acac)$_2$** and [011] axis for **L-Cu(hfac)$_2$**. In both compounds, the chains are stacked parallelly along the *b* axis (Fig. 1). For **L-Cu(acac)$_2$**, the packing of the chains in the crystal reveals the formation of 3D supramolecular motifs: upon π–π stacking and van der Waals offset interactions between pyridine/C=O groups (same plan, distances: 3.0/3.2 Å) and phenyl/CH_3 (on the consecutive plan, distances *ca.* 3.7 Å), respectively.

For **L-Cu(hfac)$_2$**, upon CH–π stacking and hydrogen offset interactions between phenyl/phenyl groups (same plan, distances: 3.6 Å) and anion π interactions between phenyl rings and halogen (phenyl/CF_3, on the consecutive plan, distances of *ca.* 3.8 Å), respectively (Fig. 2).

The distance of neighboring copper atoms bridged by one **L** ligand through the pyridine group are about 18.25 and 17.23 Å in **L-Cu(acac)$_2$** and **L-Cu(hfac)$_2$**, respectively.

The behavior of the corresponding microcrystalline powder has been tested, and XRPD measurements have been performed (Fig. 3). For **L-Cu(acac)$_2$**, the air-dried powdered samples present the same crystalline phase as calculated from XRD on single crystal data, whereas the XRPD diagram of **L-Cu(hfac)$_2$** displays the pattern of the phase revealed by XRD on single crystal together with other(s) phase(s). Attempts to separate these phases did not succeed and

Open Access Article. Published on 07 oktober 2022. Downloaded on 26.04.2026 03.20.59.
This article is licensed under a Creative Commons Attribution-NonCommercial 3.0 Unported Licence.

Table 1 Crystallographic parameters for **L-Cu(acac)$_2$**, **L-Cu(hfac)$_2$**, **L-ZnCl$_2$**, **L-CdI$_2$** and **L-CoCl$_2$** recorded at 100 K

	L-Cu(acac)$_2$	**L-Cu(hfac)$_2$**	**L-ZnCl$_2$**	**L-CdI$_2$**	**L-CoCl$_2$**
Compound formula	$C_{36}H_{34}CuN_2O_8$	$C_{36}H_{22}CuF_{12}N_2O_8$	$C_{27}H_{21}Cl_5N_2O_4Zn$	$C_{53}H_{41}Cd_2Cl_3I_4N_4O_8$	$C_{111}H_{87}Cl_{25}Co_2N_8O_{16}$
Crystal class	Monoclinic	Monoclinic	Monoclinic	Monoclinic	Monoclinic
λ, Å	0.71073	0.71073	0.71073	0.71073	0.71073
Space group	$P2_1/n$	$P2_1/n$	$C2/c$	$P2_1/n$	$C2/c$
Z	2	2	4	2	4
Cell parameters	a = 17.1498(9) Å	a = 13.7973(8) Å	a = 13.444(3) Å	a = 15.0994(15) Å	a = 23.5780(7) Å
	b = 6.2278(4) Å	b = 9.4225(6) Å	b = 11.996(2) Å	b = 7.2763(6) Å	b = 25.6210(8) Å
	c = 17.3103(9) Å	c = 14.4229(8) Å	c = 19.179(4) Å	c = 26.937(3) Å	c = 20.7280(8) Å
	α = 90°	α = 90°	α = 90°	α = 90°	α = 90°
	β = 118.78°	β = 97.481(2)°	β = 103.80(3)°	β = 100.190(2)°	β = 103.3780(13)°
	γ = 90°	γ = 90°	γ = 90°	γ = 90°	γ = 90°
V, Å^3	1620.35(16)	1859.09(19)	3003.8(11)	2912.8(5)	12181.8(7)
ρ_{calc} g cm^{-3}	1.406	1.612	1.504	1.939	1.523
Refl. meas.	13 844	18 795	21 140	16 581	30 835
Refl. [$I > 2\sigma(I)$]	3059	5221	3551	6709	7914
R_1/wR_2	0.0614/0.1515	0.0644/0.1696	0.0511/0.1469	0.0499/0.1152	0.0990/0.2730
R_1/wR_2 (all refl.)	0.0764/0.1624	0.0961/0.1919	0.0643/0.1553	0.0834/0.1310	0.1911/0.3232
Goodness-of-fit	1.055	1.053	1.041	1.022	1.009

probably result from a partial decomposition of **L-Cu(hfac)$_2$** when exposed to the air.

Structural description of 1D CP L-ZnCl$_2$

Using the already described conditions, colorless crystalline materials were obtained after few days when combining **L** with $ZnCl_2$. **L-ZnCl$_2$** crystallizes in the monoclinic $C2/c$ space group (see the crystallographic data in Table 1) and its asymmetric unit is composed of one **L**, one Zn^{2+} cations, two Cl^- anions and one disordered $CHCl_3$ solvent molecule. Zn(II) center adopts a distorted tetrahedral coordination geometry with a N_2Cl_2 environment and behaves as a two-connecting V-type node since two of its four coordination sites are occupied by two Cl^- anions with d_{Zn-Cl} = 2.2134(8) Å and Cl–Zn–Cl angle of (123.44(5)°). The two other positions are occupied by pyridine moieties with d_{Zn-N} = 2.085(2) Å and angle of N–Zn–N of 94.06(13)° (see Table 2 and also Fig. 4).

As expected from the design of the ligand **L** and the choice of $ZnCl_2$, the coordination polymer **L-ZnCl$_2$** displays a 1D dimensionality (chain running along the [101] axis) and zig-zag chains are formed, resulting from the connection through coordination bonds between **L** adopting a linear connectivity and V shaped $ZnCl_2$ metallaligands, as shown in Fig. 4.

As in the case of **L-Cu(acac)$_2$** and **L-Cu(hfac)$_2$**, in **L-ZnCl$_2$** the ligand adopts an *anti* orientation, and the pyridine and the phenyl units are perpendicular to each other.

The 1D chains are parallelly stacked along the a and b axis, as shown in Fig. 4.

Supramolecular interactions occur for **L-ZnCl$_2$**, leading to a 3D network thanks to two different π–π stacking interactions: on one hand, between pyridine rings and a carbonyl groups C=O, with distances of *ca.* 3.5 Å (on consecutive plan), respectively and on the other hand, between the phenyl groups (on the same plan), with distances of *ca.* 3.7 Å. The disordered $CHCl_3$ molecules are located between the chains and do not present any specific interaction with the network.

XRPD measurements revealed the loss of the crystallinity when the powdered sample is air-dried, accounting for the poor stability of **L-ZnCl$_2$** upon desolvation.

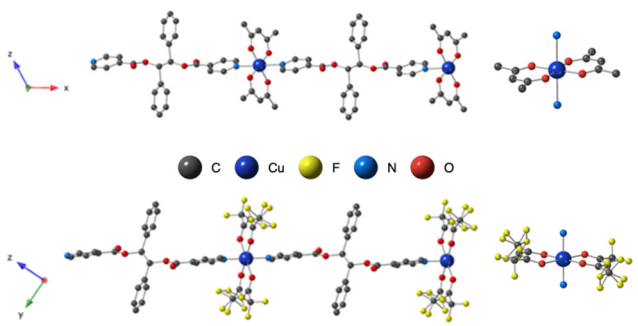

Fig. 1 Portion of the X-ray structure for **L-Cu(acac)$_2$** (top left) and **L-Cu(hfac)$_2$** (bottom left) showing the formation of the 1D neutral and linear coordination network resulting from the bridging of consecutive ligand **L** by Cu(acac)$_2$ (or Cu(hfac)$_2$) and environment around the Cu^{2+} cations. H atoms are not presented for clarity.

Structural description of 1D CP L-CdI$_2$

Using the already described conditions, crystalline materials were obtained after a few days when combining **L** with CdI_2. The single-crystal X-ray diffraction study reveals that the compound crystallizes in the monoclinic $P2_1/n$ space group (see the crystallographic data in Table 1) and its asymmetric unit is composed of one ligand **L**, one Cd^{2+} cation, two I^- anions and one disordered $CHCl_3$ solvent molecule.

A single-stranded helicoidal assembly if formed through the recognition of **L** with V shaped CdI_2 units. The Cd(II) ions, showing a distorted tetrahedral geometry, as shown in Fig. 5, are coordinated to (i) two N atoms from two consecutive **L** with Cd–N distances of 2.302(5) and 2.298(5) Å and N–Cd–N

 This journal is © The Royal Society of Chemistry 2022

Open Access Article. Published on 07 oktober 2022. Downloaded on 26.04.2026 03.20.59.
This article is licensed under a Creative Commons Attribution-NonCommercial 3.0 Unported Licence.

Table 2 Selected bond lengths (Å) around the M(II) ions for **L-Cu(acac)$_2$**, **L-Cu(hfac)$_2$**, **L-ZnCl$_2$**, **L-CdI$_2$** and **L-CoCl$_2$**

L-Cu(acac)$_2$		**L-Cu(hfac)$_2$**		**L-ZnCl$_2$**		**L-CdI$_2$**		**L-CoCl$_2$**	
Cu–O4	1.933(2)	Cu–O4	1.9987(18)	Zn–N1	2.085(2)	Cd–N1	2.298(5)	Co2–N3	2.175(4)
Cu–O3	1.970(2)	Cu–N1	2.0212(19)	Zn–Cl1	2.2134(8)	Cd–N2	2.302(5)	Co1–N1	2.201(4)
Cu–N1	2.489(3)	Cu–O3	2.260(2)			Cd–I2	2.6728(6)	Co1–N2	2.210(4)
						Cd–I3	2.7195(7)	Co2–N4	2.260(4)
								Co1–Cl1	2.4175(14)
								Co2–Cl2	2.4421(14)

angle of 95.77(17)° and (ii) two iodide anions, with Cd–I bond lengths close to 2.7 Å and I–Cd–I angle of 129.6° (see Table 2).

Unlike in **L-Cu(acac)$_2$**, **L-Cu(hfac)$_2$** and **L-ZnCl$_2$**, **L** adopts a *syn-syn-syn* conformation, and the pyridine groups are almost parallel (dihedral angle 18.85°) and convergently oriented towards the concave face of the backbone. The two pyridine units are in *anti* positions of the phenyl units while the dihedral angle between the two phenyl rings is 45.74°, as shown Fig. 5.

As shown in Fig. 5, the helicoidal chains are running along the *b* axis.

The distance between two consecutive Cd^{2+} cations is ca 8.2 Å. The fragment that determines the pitch (7.3 Å) of the helix is composed of two CdI_2 and two ligands **L**. The system is achiral, since both (50/50) types of helices (*M* and *P*) are present in the crystal.

The packing of the chains in the *xOz* plane is shown in Fig. 6. The disordered $CHCl_3$ molecules are located between the chains with no specific interaction with the network.

XRPD measurements revealed the loss of the crystallinity when the powdered sample is air-dried and desolvated, accounting for the poor stability of **L-CdI$_2$** in air.

Structural description for cobalt 2D CP L-CoCl$_2$

Using the already described conditions, crystalline materials were obtained after a few days when combining **L** with $CoCl_2$. The X-ray diffraction on single crystal study reveals that **L-CoCl$_2$** is crystallizing in the monoclinic *C*2/*c* space group (see the crystallographic data in Table 1) and its asymmetric unit is composed of four ligands **L**, two Co^{2+} cations, four Cl^- anions and seven $CHCl_3$ solvent molecules. The obtained coordination pattern results from the recognition of $CoCl_2$ units by **L** through the formation of coordination bonds. A 2D grid-type neutral architecture is formed by the connection of four ligands **L** by $CoCl_2$ complexes behaving as 4-connected nodes (Fig. 7). The Co(II) centers, adopting a

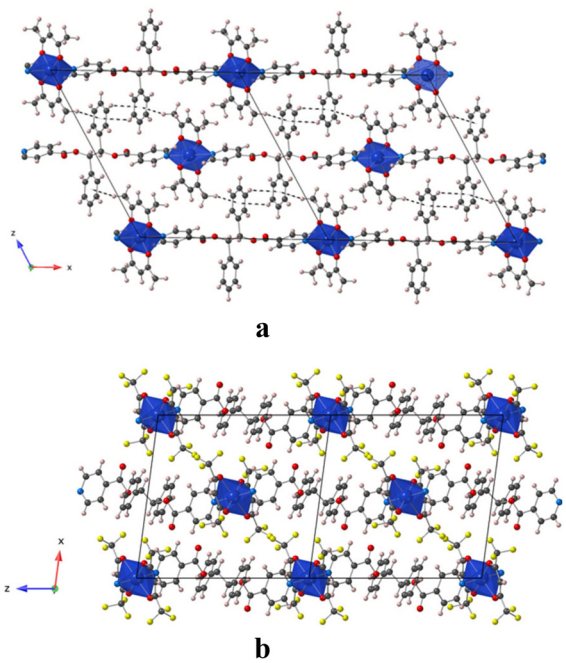

Fig. 2 Portion of the X-ray structure of **L-Cu(acac)$_2$** (a) and **L-Cu(hfac)$_2$** (b) showing the packing of consecutive chains in the *zOx* plane.

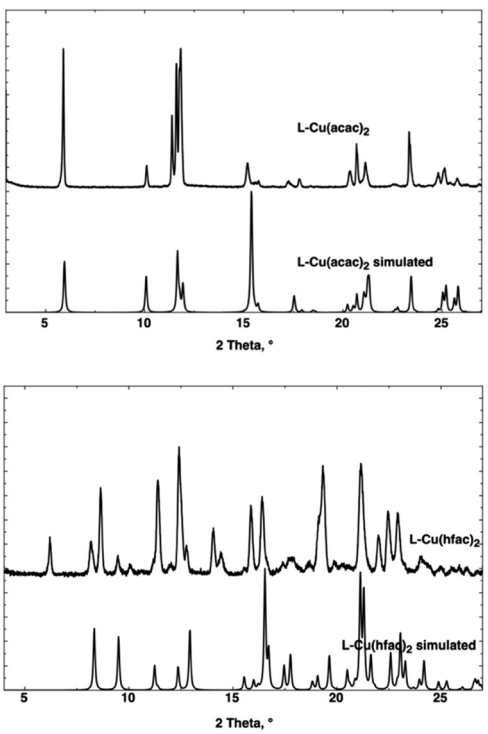

Fig. 3 For **L-Cu(acac)$_2$** (bottom) and **L-Cu(hfac)$_2$** (top), XRPD diagrams of the air-dried compounds, compared with the simulated phases obtained for **L-Cu(acac)$_2$** and **L-Cu(hfac)$_2$** from X-ray diffraction data.

Open Access Article. Published on 07 oktober 2022. Downloaded on 26.04.2026 03.20.59.
This article is licensed under a Creative Commons Attribution-NonCommercial 3.0 Unported Licence.

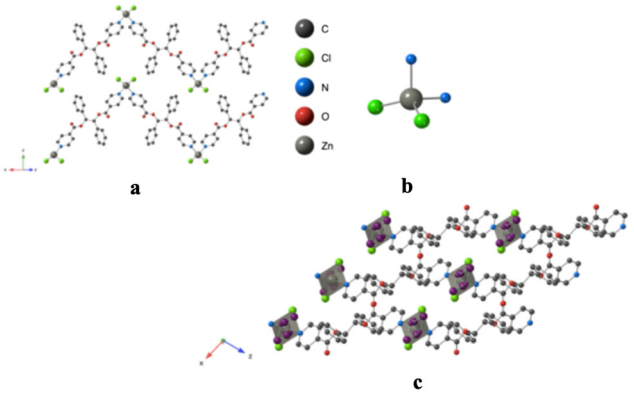

Fig. 4 For **L-ZnCl$_2$**, portions of the X-ray structure showing a) the formation of the 1D zig-zag type coordination polymer, b) environment around the Zn^{2+} cations and c) packing of consecutive networks in the *xOz* plane. Disordered chloroform solvent molecules are represented in purple. H atoms are not represented for clarity.

distorted octahedral geometry, are linked to four N from four different ligands, occupying the apices of the square base of the octahedron through N–Co coordination bonds (d_{Co-N}: 2.201(4)–2.210(4) Å, see Table 2 and Fig. 7). The two Cl^- anions are occupying the apical positions with d_{Co-Cl} distances close to 2.4 Å.

Within the 2D network, the two phenyl moieties of the ligand are nearly parallel (dihedral angle 3.2°) while the dihedral angle of the two pyridines is 73.1°.

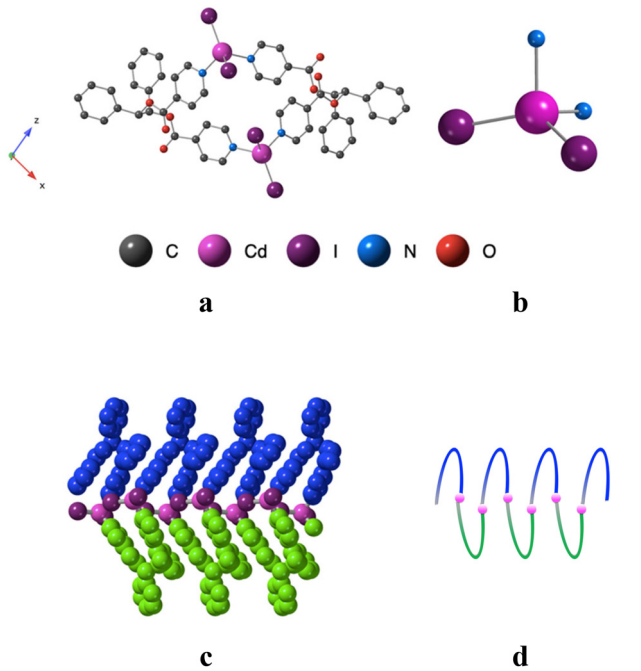

Fig. 5 For **L-CdI$_2$** a), portion of the X-ray structure of **L-CdI$_2$** b) environment around the Cd^{2+} cations c) the 1D helicoidal coordination polymer, projection in the *xOz* plane, and d) schematic representation of the helical 1D structure. H atoms and chloroform solvent molecules are not represented for clarity.

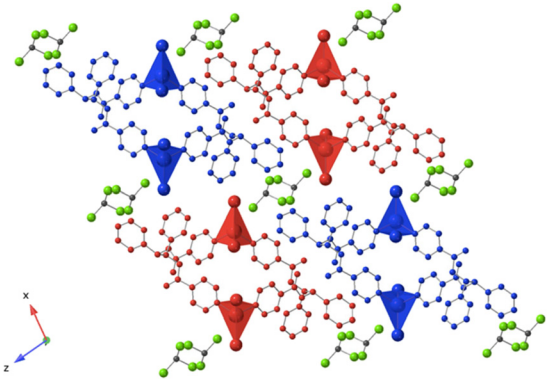

Fig. 6 Portion of the X-ray structure of **L-CdI$_2$** showing the packing of consecutive 1D zig-zag type networks in the *xOz* plane. H atoms are not represented for clarity.

As shown in Fig. 8, the grids are stacked parallelly along the *c* axis. But they do not superimpose and a network composed of four different grids is thus forming a dense network, without any porosity.

Within the 2D sheet, the consecutive Co^{2+} cations are distant of *ca.* 17.40 Å.

Consecutive 2D-grids are parallel but shifted (Fig. 8b) with no specific interactions between grids. The distance between consecutive layers, with respect to the mean planes formed by the 4 connected Co(II) centers, is *ca.* 5 Å.

The $CHCl_3$ molecules are located between the layers and interact with one apical Cl^- anion (3.55 Å) and H atoms of either on adjacent Py or phenyl moieties ($d_{CHCl_3\cdots Py}$ = 3.4 Å or $d_{CHCl_3\cdots Ph}$ = 3.2 Å).

The XRPD measurements also revealed the loss of the crystallinity when the powdered sample is air-dried desolvated, accounting for the poor stability of **L-CoCl$_2$** in air.

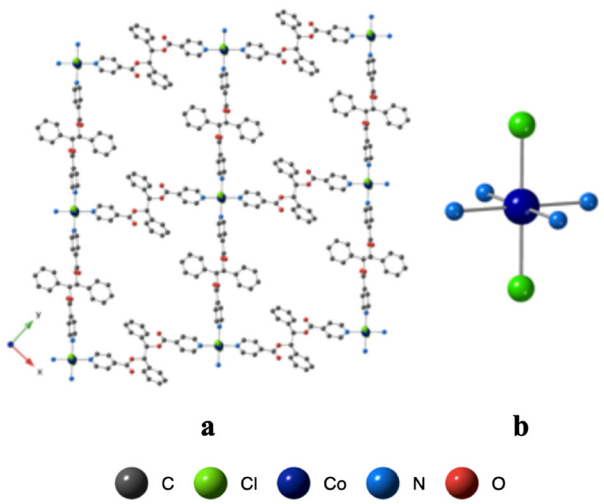

Fig. 7 Portions of the X-ray structure of **L-CoCl$_2$** showing the formation of grids between the connection of L with $CoCl_2$ metallaligands (a) and environment around the Co^{2+} cations (b). H atoms and chloroform solvent are not represented for clarity.

This journal is © The Royal Society of Chemistry 2022

Open Access Article. Published on 07 oktober 2022. Downloaded on 26.04.2026 03.20.59.
This article is licensed under a Creative Commons Attribution-NonCommercial 3.0 Unported Licence.

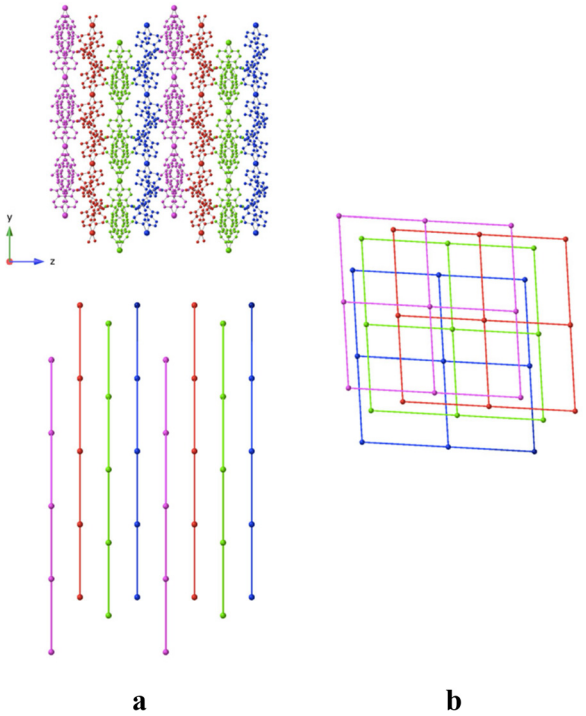

Fig. 8 For **L-CoCl$_2$**, schematic representation of the packing showing a) the parallel 2D grids in the *yOz* plane and b) the superposition of the grids along the *c* axis, leading to a network presenting no porosity.

Discussion

As revealed by the above shown results, the flexibility of the used ligand **L**, combined with rigid metallaligands $Cu^{II}(acac)_2$, $Cu^{II}(hfac)_2$, $Zn^{II}Cl_2$, $Cd^{II}I_2$ or $Co^{II}Cl_2$, leads to a large diversity of coordination polymers. This illustrates the powerful approach of using flexible ligands to obtain CPs of targeted dimensionalities (from 1D to 2D) and also various geometries (for 1D CP: linear, zig-zag or helicoidal chains), as shown in Table 3.

We have shown that **L** can adopt two conformations depending on the used metal connector: *syn-syn-syn* and *anti-anti-anti*. In the first case, the two pyridine units adopt a completely opposite direction (180°). This conformation has been observed for **L-ZnCl$_2$**, **L-Cu(acac)$_2$**, **L-Cu(hfac)$_2$** and **L-CoCl$_2$**. Regarding the second conformation, even if it is energetically less favorable than the previous one it has been observed in the case of **L-CdI$_2$**. In this case, the two pyridines adopted a convergently oriented towards the concave face of the backbone (18.85°).

Experimental

Synthesis

All reagents were purchased from commercial sources and used without further purification.

Synthesis of 1,2-diphenylethane-1,2-diyl diisonicotinate (L)

A solution (40 ml) of *meso*-1,2-diphenyl-1,2-ethanediol (0.5 g, 2.3 mmol) in dry THF, isonicotinoyl chloride, hydrochloride (1 g, 5.6 mmol, 2.5 equiv) were placed into a vial and stirred at room temperature. After 15 min, Et_3N (4 ml) was added to the solution, and the stirring was further continued under reflux overnight.

After evaporation to dryness, the saturated aqueous solution of Na_2CO_3 (40 ml) was added to the residue then the mixture was extracted with CH_2Cl_2 (3 × 30 ml). The organic layer was dried ($MgSO_4$), and the solvent was removed. The remaining solid was purified by column chromatography (SiO_2, eluent CH_2Cl_2 then CH_2Cl_2/MeOH 1% then 2%) to yield a white solid (0.75 g, 77% yield).

^{1}H-NMR (500 MHz, $CDCl_3$, 25 °C) δ (ppm): 8.75 (d, 4H, J = 9 Hz), 7.75 (d, 4H, J = 9 Hz), 7.29 (m, 6H), 7.24 (m, 4H), 6.45 (s, 2H); ^{13}C-NMR (125 MHz, $CDCl_3$, 25 °C) δ (ppm): 163.8, 150.8, 136.8, 134.9, 129.0, 128.4, 127.4, 122.8. Elem. anal. calc. for $C_{26}H_{20}N_2O_4$: C, 73.57%; H, 4.75%; N, 6.60%; found: C, 73.65%; H, 4.85%; N, 6.55%.

Crystallization conditions for CPs

In a crystallization tube (height = 12 cm, diameter = 0.4 cm), at room temperature upon slow diffusion of a EtOH (3 ml)

Table 3 Geometrical features of the CPs **L-Cu(acac)$_2$**, **L-Cu(hfac)$_2$**, **L-ZnCl$_2$**, **L-CdI$_2$** and **L-CoCl$_2$**

	L-Cu(acac)$_2$	L-Cu(hfac)$_2$	**L-ZnCl$_2$**	**L-CdI$_2$**	**L-CoCl$_2$**
Conformation	*anti-anti-anti*	*anti-anti-anti*	*anti-anti-anti*	*syn-syn-syn*	*anti-anti-anti*
Dimensionality and geometry of obtained CP Schematic representation	1D-linear	1D-linear	1D-zig-zag	1D-helicoidal	2D-grid

Open Access Article. Published on 07 oktober 2022. Downloaded on 26.04.2026 03.20.59.
This article is licensed under a Creative Commons Attribution-NonCommercial 3.0 Unported Licence.

solution of metal salt (4 mg) into a $CHCl_3$ solution (1.5 ml) of **L** (3 mg), crystals were obtained after *ca.* 24–48 h.

To characterize the bulk material, EA were performed on all crystals. However, except, for **L-Cu(acac)$_2$** and **L-Cu(hfac)$_2$**, since all other crystalline materials studied contain solvent molecules, the data obtained for **L-ZnCl$_2$**, **L-CdI$_2$** and **L-CoCl$_2$** were erratic and not reproducible.

L-Cu(acac)$_2$. Elem. anal. calc. for $C_nH_nN_nO_nCu_n$: C, 63.01%; H, 4.99%; N, 4.08%; found: C, 62.43%; H, 5.05%; N, 3.90%.

L-Cu(hfac)$_2$. Elem. anal. calc. for $C_nH_nN_nO_nF_nCu_n$: C, 47.93%; H, 2.46%; N, 3.11%; found: C, 48.70%; H, 2.56%; N, 3.02%.

Materials

^{1}H-NMR and ^{13}C-NMR spectra were recorded at room temperature on Bruker (400 or 500 MHz) NMR spectrometers by the shared NMR Service of the Faculty of Chemistry of Strasbourg University.

Elemental analyses were performed by the Service de Microanalyses de la Fédération de Recherche Chimie, Université de Strasbourg, Strasbourg, France.

Crystal X-ray data collection

Data were collected at 173(2) K on a Bruker SMART CCD Diffractometer equipped with an Oxford Cryosystem liquid N_2 device, using graphite-monochromated Mo Kα (λ = 0.71073 Å) radiation. For all structures, diffraction data were corrected for absorption and structural determination was achieved using the APEX (1.022) package. All hydrogen atoms have been calculated except those connected to disordered atoms.

CCDC reference numbers 2189978 (**L-CoCl$_2$**), 2189979 (**L-ZnCl$_2$**), 2189980 (**L-Cu(acac)$_2$**), 2189981 (**L-Cu(hfac)$_2$**) and 2189982 (**L-CdI$_2$**).

XRPD measurements

Powder diffraction studies (PXRD) diagrams for air-dried powdered samples were collected on polycrystalline powder at the room temperature (293(2) K), on a Bruker D8 diffractometer using monochromatic Cu-Kα radiation with a scanning range between 2° and 40° at a scan step size of 2° min^{-1} and sample holder rotation at 15 rpm.

Conclusions

The synthesis of a new flexible bis pyridine containing ligand **L** (1,2-diphenylethane-1,2-diyl diisonicotinate) based on the 1,2-diphenylethane skeleton was achieved in 77% yield. Combinations of this new ligand, behaving as a bis-monodentate flexible ligand with $Cu(acac)_2$, $Cu(hfac)_2$, $ZnCl_2$, CdI_2 or, $CoCl_2$, leads to a large diversity of coordination polymers. The used metallaligands are behaving as a two-connecting linear ($Cu(acac)_2$, $Cu(hfac)_2$) or V-shape ($ZnCl_2$, CdI_2) nodes, leading to the formation of a 1D molecular coordination wire while, $CoCl_2$ is offering four free connecting sites, leading to a 2D grid-type. In addition, the flexibility of the ligands allows to adopt different conformation, here illustrated by *anti-anti-anti* or *syn-syn-syn* It should be noted that the design principle allows us to predict only the connectivity pattern and geometry of the 1D or 2D networks but not their packing that leads to crystal formation due to the ligand flexibility.

Conflicts of interest

There are no conflicts to declare.

Acknowledgements

Financial support from the University of Strasbourg and the CNRS are also acknowledged.

Notes and references

1 B. F. Abrahams, B. F. Hoskins and R. Robson, A new type of infinite 3D polymeric network containing 4-connected, peripherally-linked metalloporphyrin building blocks, *J. Am. Chem. Soc.*, 1991, **113**, 3606–3607.
2 J. R. Long and O. M. Yaghi, The pervasive chemistry of metal–organic frameworks, *Chem. Soc. Rev.*, 2009, **38**, 1213–2114.
3 W. L. Leong and J. J. Vittal, One-Dimensional Coordination Polymers: Complexity and Diversity in Structures, Properties, and Applications, *Chem. Rev.*, 2011, **111**, 688–764.
4 H. C. J. Zhou and S. Kitagawa, Metal-Organic Frameworks (MOFs), *Chem. Soc. Rev.*, 2014, **43**, 5415–5418.
5 M. Dincă and J. R. Long, Porous framework chemistry special issue, *Chem. Rev.*, 2020, **120**, 8037–8038.
6 R. P. Feazell, C. E. Carson and K. K. Klausmeyer, Anion-dependent silver(I) coordination polymers of the tridentate pyridylphosphonite: $PPh(3\text{-}OCH_2C_5H_4N)_2$, *Inorg. Chem.*, 2005, **44**, 996–1005.
7 X. Cui, A. N. Khlobystov, X. Chen, D. H. Marsh, A. J. Blake, W. Lewis, N. R. Champness, C. J. Roberts and M. Schröder, Dynamic Equilibria in Solvent-Mediated Anion, Cation and Ligand Exchange in Transition-Metal Coordination Polymers: Solid-State Transfer or Recrystallisation?, *Chem. – Eur. J.*, 2009, **15**, 8861–8873.
8 S. Shimomura, N. Yanai, R. Matsuda and S. Kitagawa, Impact of Metal-Ion Dependence on the Porous and Electronic Properties of TCNQ-Dianion-Based Porous Coordination Polymers, *Inorg. Chem.*, 2011, **50**, 172–177.
9 L. Li, S. Wang, T. Chen, Z. Sun, J. Luo and M. Hong, Solvent-Dependent Formation of Cd(II) Coordination Polymers Based on a C_2-Symmetric Tricarboxylate Linker, *Cryst. Growth Des.*, 2012, **12**, 4109–4115.
10 J. W. Shin, Y. H. Lee, J. Harrowfield, S. Hayami and Y. Kim, Anion-dependent interpenetration in lattices of Ag(I) complexes of a divergent quaterpyridine-donor ligand, *Polyhedron*, 2017, **130**, 94–99.

 This journal is © The Royal Society of Chemistry 2022

Open Access Article. Published on 07 oktober 2022. Downloaded on 26.04.2026 03.20.59.
This article is licensed under a Creative Commons Attribution-NonCommercial 3.0 Unported Licence.

11 L. Carlucci, G. Ciani and D. M. Proserpio, Polycatenation, polythreading and polyknotting in coordination network chemistry, *Coord. Chem. Rev.*, 2003, **246**, 247–289.
12 G. Férey, C. Mellot-Draznieks, C. Serre and F. Millange, Crystallized Frameworks with Giant Pores: Are There Limits to the Possible?, *Acc. Chem. Res.*, 2005, **38**, 217–225.
13 S. Kitagawa and K. Uemura, Dynamic porous properties of coordination polymers inspired by hydrogen bonds, *Chem. Soc. Rev.*, 2005, **34**, 109–119.
14 D. Maspoch, D. Ruiz-Molina and J. Veciana, Old materials with new tricks: multifunctional open-framework materials, *Chem. Soc. Rev.*, 2007, **36**, 770–818.
15 C. Janiak and J. K. Vieth, MOFs, MILs and more: concepts, properties and applications for porous coordination networks (PCNs), *New J. Chem.*, 2010, **34**, 2366–2388.
16 M. Yoon, R. Srirambalaji and K. Kim Homochiral, Metal–Organic Frameworks for Asymmetric Heterogeneous Catalysis, *Chem. Rev.*, 2012, **112**, 1196–1231.
17 Y. Shi, A.-F. Yang, C.-S. Cao and B. Zhao, Applications of MOFs: Recent advances in photocatalytic hydrogen production from water, *Coord. Chem. Rev.*, 2019, **390**, 50–75.
18 G. R. Desiraju, Crystal Engineering: From Molecule to Crystal, *J. Am. Chem. Soc.*, 2013, **135**, 9952–9967.
19 Y. Zhao, K. Li and J. Li, Solvothermal Synthesis of Multifunctional Coordination Polymers, *Z. Naturforsch., B: J. Chem. Sci.*, 2010, **65**, 976–998.
20 H. Wu, X.-L. Lü, C.-L. Yang, C.-X. Dong and M.-S. Wu, Diverse topologies of seven d10 coordination polymers constructed from a long ligand and different carboxylates, *CrystEngComm*, 2014, **16**, 992–1000.
21 A. Y. Chahine, D. R. Turner and S. R. Batten, Crystal engineering of coordination polymers using flexible tetracarboxylate linkers with embedded cyclohexyldiamine cores, *CrystEngComm*, 2021, **23**, 569–590.
22 Y.-Q. Zheng, J.-L. Lin and Z.-P. Kong, Coordination Polymers Based on Cobridging of Rigid and Flexible Spacer Ligands: Syntheses, Crystal Structures, and Magnetic Properties of $[Mn(bpy)(H_2O)(C_4H_4O_4)]\cdot 0.5bpy$, $Mn(bpy)(C_5H_6O_4)$, and $Mn(bpy)(C_6H_8O_4)$, *Inorg. Chem.*, 2004, **43**, 2590–2596.
23 C.-L. Zhang, H. Xu, X.-W. Song, Y. Meng and J.-J. Chen, Three d10 coordination polymers based on rigid ligands with flexible functional groups: Syntheses, structures and luminescence, *Inorg. Chem. Commun.*, 2017, **84**, 229–233.
24 P. Larpent, A. Jouaiti, N. Kyritsakas and M. W. Hosseini, Molecular tectonics: homochiral 1D and 2D cadmium based coordination networks, *CrystEngComm*, 2019, **21**, 2534–2540.
25 Z. Tian, J. Lin, Y. Su, L. Wen, Y. Liu, H. Zhu and Q.-J. Meng, Flexible Ligand, Structural, and Topological Diversity: Isomerism in $Zn(NO_3)_2$ Coordination Polymers, *Cryst. Growth Des.*, 2007, **7**, 1863–1867.
26 A. J. Emerson, C. S. Hawes, G. P. Knowles, A. L. Chaffee, S. R. Batten and D. R. Turner, Coordination polymers from a flexible alkyldiamine-derived ligand, *CrystEngComm*, 2017, **19**, 5137–5145.
27 A. Lalegani, M. K. Sardashti, R. Gajda and K. Woźniak, Synthesis and characterization of two new zinc(II) coordination polymers with bidentate flexible ligands: Formation of a 2D structure with (44.62)-sql topology, *J. Mol. Struct.*, 2017, **1149**, 777–784.
28 L.-C. Song, W.-X. Zhang and J.-Y. Wang, Two Novel One-dimensional Coordination Polymers $[Cu_2(m\text{-}Br)_2(pcaede)_2 2\text{-}H_2O]_n$ and $[Cu_2(m\text{-}Br)_2(pcaede)_2 0.5THF 0.5H_2O]_n$ Formed via Self-assembly of 4-Pyridinecarboxylic Acid 1,2-Ethyanediyl Ester (pcaede) with Copper(I) Bromide, *Transition Met. Chem.*, 2002, **27**, 526–531.
29 L.-C. Song, W.-X. Zhang and Q.-M. Hu, Syntheses and Characterizations of Novel One-dimensional Coordination Polymers Self-assembled from $Co(NCS)_2$ and Flexible Diester-bridged Pyridine-based Ligands, *Chin. J. Chem.*, 2002, **20**, 1421–1429.
30 P. Grosshans, A. Jouaiti, V. Bulach, J.-M. Planeix, M. W. Hosseini and N. Kyritsakas, Design and Structural Analysis of Metallamacrocycles Based on a Combination of Ethylene Glycol Bearing Pyridine Units with Zinc, Cobalt and Mercury, *Eur. J. Inorg. Chem.*, 2004, 453–458.
31 B. Chatterjee, J. C. Noveron, M. J. E. Resendiz, J. Liu, T. Yamamoto, D. Parker, M. Cinke, C. V. Nguyen, A. M. Arif and P. J. Stang, Self-Assembly of Flexible Supramolecular Metallacyclic Ensembles: Structures and Adsorption Properties of Their Nanoporous Crystalline Frameworks, *J. Am. Chem. Soc.*, 2004, **126**, 10645–10656.
32 A. Y. Robin, J. L. S. Doimeadios, A. Neels, T. V. Slenters and K. M. Fromm, Structure–property relationships: Polymorphism, solvates, and clay behavior in the one-dimensional coordination polymer chains $[Ag(L)(NO_3)](H_2O)_n$, L = ethanediyl bis(isonicotinate), n = 0, and 2, *Inorg. Chim. Acta*, 2007, **360**, 212–220.
33 K. M. Fromm, J. L. Sagué and A. Y. Robin, Silver coordination polymers with isonicotinic acid derived short polyethylene glycol–Synthesis, structures, anion effect and solution behavior, *Inorg. Chim. Acta*, 2013, **403**, 2–8.
34 J. Yan, M. Qi, X. Haitao, S. Xiaoqiang and W. Xin, 1,2-Diphenylethane-1,2-diyl diisonicotinate monohydrate, *Acta Crystallogr., Sect. E: Struct. Rep. Online*, 2008, **64**, o1992.
35 H. R. Khavasi and B. M. M. Sadegh, Isostructural Mercury Coordination Polymers with Amide Junction: Interplay of Coordination and π–π Stacking, *Cryst. Growth Des.*, 2012, **12**, 4798–4804.